Dynamics and Reactivity of Trapped Electrons on Supported Ice Crystallites

JULIA STÄHLER,*,†,‡ CORNELIUS GAHL,‡,§ AND
MARTIN WOLF†,‡

†Department of Physical Chemistry, Fritz-Haber-Institut der Max-Planck-Gesellschaft, Faradayweg 4-6, 14195 Berlin, Germany, ‡Department of Physics, Freie Universität Berlin, Arnimallee 14, 14195 Berlin, Germany, and §Max-Born-Institute Berlin, Max-Born-Str. 2 A, 12489 Berlin, Germany
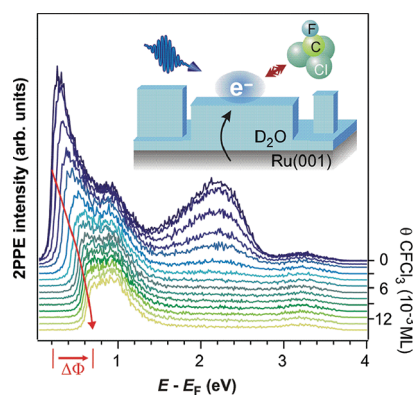
CONSPECTUS

The solvation dynamics and reactivity of localized excess electrons in aqueous environments have attracted great attention in many areas of physics, chemistry, and biology. This manifold attraction results from the importance of water as a solvent in nature as well as from the key role of low-energy electrons in many chemical reactions. One prominent example is the electron-induced dissociation of chlorofluorocarbons (CFCs). Low-energy electrons are also critical in the radiation chemistry that occurs in nuclear reactors.

Excess electrons in an aqueous environment are localized and stabilized by the local rearrangement of the surrounding water dipoles. Such solvated or hydrated electrons are known to play an important role in systems such as biochemical reactions and atmospheric chemistry. Despite numerous studies over many years, little is known about the microscopic details of these electron-induced chemical processes, and interest in the fundamental processes involved in the reactivity of trapped electrons continues.

In this Account, we present a surface science study of the dynamics and reactivity of such localized low-energy electrons at D_2O crystallites that are supported by a Ru(001) single crystal metal surface. This approach enables us to investigate the generation and relaxation dynamics as well as dissociative electron attachment (DEA) reaction of excess electrons under well-defined conditions. They are generated by photoexcitation in the metal template and transferred to trapping sites at the vacuum interface of crystalline D_2O islands. In these traps, the electrons are effectively decoupled from the electronic states of the metal template, leading to extraordinarily long excited state lifetimes on the order of minutes. Using these long-lived, low-energy electrons, we study the DEA to $CFCl_3$ that is coadsorbed at very low concentrations ($\sim 10^{12}$ cm^{-2}). Using rate equations and direct measurement of the change of surface dipole moment, we estimated the electron surface density for DEA, yielding cross sections that are orders of magnitude higher than the electron density measured in the gas phase.

1. Intoduction

The solvation dynamics and reactivity of localized excess electrons in an aqueous environment has attracted great attention in a large number of areas in physics, chemistry, and biology. This manifold attraction results from the importance of water as a solvent in nature as well as from the key role of low-energy electrons in many chemical reactions.[1] One prominent example is the electron-induced dissociation of chlorofluorocarbons (CFCs), whose role in the enhancement of ozone layer depletion is under debate,[2−4] but low-energy electrons are also critical in the radiation chemistry that occurs, for instance, in nuclear reactors.[5]

In the polar environment of liquid water or water-ice, excess electrons tend to localize, being stabilized by re-arrangements of the hydrogen bonded network. The widely accepted *cavity model*, in which the electron is surrounded by (typically six) water molecules of the first solvation shell,[6,7] has recently been questioned by molecular dynamics simulations that predict hydration of the electron even in denser regions of liquid water,[8] launching a new

debate[9−12] about the character of the solvation site in liquid water. Somewhat connected, also the trapping site of excess electrons in water cluster anions has been controversially discussed in the past,[13−18] in particular with regard to the question under which circumstances the electron is bound in the bulk or on the surface of the gas phase clusters. Besides liquid water and gas phase anion cluster studies, the solvation of excess electrons has also been subject of surface science studies in which H_2O and D_2O ice was investigated on different substrates,[19−23] which would not have been possible without thorough characterization and understanding of the ice structure and morphology on single crystal surfaces.[24−27] The susceptibility of supported ice-electron complexes to dissociative electron attachment (DEA) of chlorofluorocarbons has previously been studied by Lu and Sanche (see, e.g, ref 28 and references therein). They focused on the enhancement of DEA of different CFCs due to the presence of polar molecules by systematic studies on rare gas buffer layers. Furthermore, Ryu et al. found that solvated electrons in ice films on a silver crystal can drive the DEA reaction of $CFCl_3$.[29]

Investigating the ground and excited state properties of the solvated (hydrated) electron is crucial for a sound understanding of chemical reactions induced by such low-energy electrons. In the case of water cluster anions[7,15,30,31] and liquid water,[8,32−36] most investigations focused on the relaxation dynamics of the system after photoexcitation from the *s*-type ground to the *p*-type excited state. On the other hand, the time-resolved surface science studies of amorphous ice on metal and semiconductor surfaces[19−21] have been focusing on the properties of excess electrons in a polar, aqueous environment during and right after the initial injection of the electron from the respective template. However, in line with most studies of electron dynamics at (polar) molecule−metal interfaces,[37−40] the equilibrium solvated ground state is never reached in these systems due to the finite excited state lifetime on femto- or picosecond time scales. In other words, besides acting as the source of electrons, the substrate also presents a *sink* for the excess electrons, limiting their lifetime and availability for chemical reactions.[29] In part, this has been circumvented by decoupling by rare gas buffer layers.[3]

The recent discovery of much longer living electrons at the vacuum interface of supported ice crystallites with excited state lifetimes up to minutes[41,42] now crosses the bridge between the surface science approach and the gas phase cluster anion studies: The excess electrons are created by charge transfer from the metal substrate as in previous
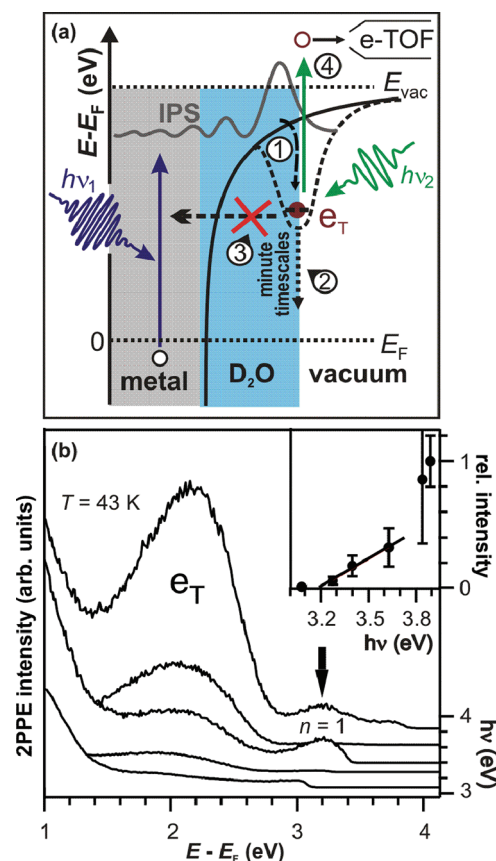

FIGURE 1. (a) Elementary processes involved in electron trapping at the ice−metal interface. Photoinjected electrons localize at pre-existing sites at the vacuum interface of the D_2O crystallites (1) and undergo further solvation that increases their binding energy with respect to vacuum (2). The population of this trapped electron state e_T is further reduced by transfer back to the metal at a characteristic time scale τ (3) as well as depopulation by photoemission (4). (b) Monochromatic 2PPE spectra recorded with different UV photon energies. As evident by the photon energy dependence of the e_T intensity (inset), the population of the trapped electron state e_T requires excitation via the $n = 1$ image potential state at $E − E_F = 3.2$ eV. Its photostationary population increases with photon energy.

surface science studies; however, they are trapped at pre-existing sites at the *surface* of the ice crystallites. In these deep traps, the electrons are strongly screened and very efficiently decoupled electronically from the metal. In this way, it is possible to observe their relaxation dynamics toward the ground state over 17 orders of magnitude in time, from the femtosecond time regime up to minutes.[41]

In this Account, we will discuss the elementary processes in the formation and decay of such trapped electrons on ice crystallites as well as their reactivity. Fluence-dependent experiments provide information about the density of trapped electrons at supported D_2O crystallites and their relaxation as a function of time. Moreover, it will be shown that these low-energy surface-bound electrons react very

efficiently with $CFCl_3$ even at very low concentrations. These observations directly prove the high reactivity of trapped electrons at ice crystallites with CFCs and may be of relevance for electron-induced reactions at ice particles in polar stratospheric clouds.

2. Electron Capture at Ice Crystallites on Metal Surfaces

Figure 1a displays schematically the elementary processes involved in excess electron capture and relaxation at ice crystallites adsorbed on a metal substrate,[43] which are probed by time-resolved two-photon photoelectron (2PPE) spectroscopy. Thereby, electrons are excited by UV photon absorption in the metal ($h\nu_1$). This brings the system in a nonequilibrium condition and launches relaxation dynamics. These are monitored by subsequent photoemission of the excited state population by time-delayed photons $h\nu_2$ as described in detail in refs 41 and 44. For crystalline ice at single crystal metal surfaces (here Ru(001)) image potential states (IPS) are formed at the interface, exhibiting a spatial overlap with the substrate as well as with the conduction band of ice. These delocalized states mediate the charge transfer to local configurations that trap the electrons close to the ice−vacuum interface (see process (1) in Figure 1). Localization of the excess charge induces a reorganization of surrounding polar water molecules stabilizing the trapped charge and increasing its binding energy (process (2)). The time scale of this solvation process depends strongly on the sample temperature.[41] At all times, the population of trapped electron decays by tunnelling through the ice to the unoccupied states of the metal substrate (process (3)); however, in the case of crystalline D_2O, the decay rate is strongly reduced by efficient dipole screening of the trapped electron by the trapping site. Besides these intrinsic processes, the population of e_T is further depleted by photoemission upon absorption of another UV or visible photon (4).

In the following, we discuss all these processes in more detail. Figure 1b shows monochromatic 2PPE spectra taken at a temperature of 43 K and normalized to the photon flux. They are plotted as a function of energy of the intermediate state in the 2PPE process and have a vertical offset according to the photon energy used. A pronounced peak of transiently populated electronic states is observed at 2.2 eV above the Fermi level. These states are normally unoccupied, but *bound*, as they clearly lie below the vacuum level of the sample (work function $\Phi = 3.9$ eV). As shown further below, they stem from localized electrons that are trapped at the ice−vacuum interface. Their spectral signature (e_T) is only observed if the
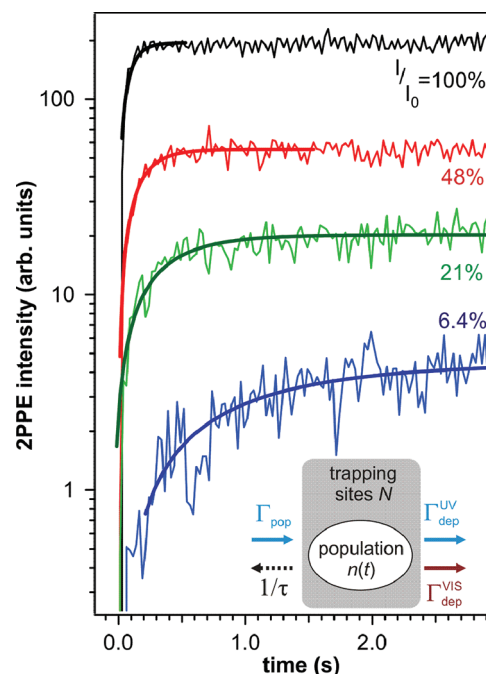

FIGURE 2. 2PPE intensity in the energy range of e_T as a function of illumination time for different UV intensities realized by attenuation of the full laser beam ($h\nu = 3.9$ eV). The bold lines represent exponential fits to extract the rise time and the asymptotic intensity in the photo-stationary state. A rate equation model (inset), taking into account the different population and depopulation channels, reproduces the population dynamics of the trapping sites and enables the deduction of their total density.

photon energy exceeds 3.2 eV, and its intensity increases with photon energy as illustrated by the inset of Figure 1b. This threshold energy corresponds to the photon energy needed to populate the first image potential state (IPS) on the ice-covered Ru(001) surface. Since there is no electronic transition at this energy within the ice and no specific resonance related to transitions in the substrate, we conclude that the image potential states, in particular the energetically lowest one, serve as charge transfer states.

From here, electrons can be captured at specific trapping sites. As the lifetime of the IPS is below 10 fs, these sites must exist before excitation and are not dynamically formed by self-trapping.[41] The localized electronic states in these traps are extremely well decoupled from the metal substrate and result in lifetimes ranging up to minutes. This exceeds by far the time between subsequent laser pulses in the 2PPE given by the repetition rate of the laser (200 kHz) so that the population accumulates over many laser pulses until a photostationary equilibrium of population, charge transfer and photoemission is reached.

In Figure 2, the photoemission intensity of e_T is plotted as a function of UV illumination time for a series of excitation

fluences. In all cases, the 2PPE intensity rises and approaches exponentially a saturation value. The exponential rise time (τ_r) and asymptotic intensity both depend nearly linearly on the average laser intensity in the regime of $\sim$0.01 to 1 W/cm^2.[45] The build-up of this photostationary state can be well described by a rate equation taking into account the optical population with the rate Γ_{pop} and the depopulation due to electron decay toward the substrate with $1/\tau$ as well as photoemission with Γ_{dep} as sketched in the inset of Figure 2.[45,46] Introducing additional laser pulses at a photon energy below 3.2 eV, that is, insufficient to form trapped electrons, but sufficient to probe them, allows us to estimate the density of trapping sites on the ice crystallites to be on the order of $N = 2.5 \times 10^{11}$ cm^{-2} (assuming a detection probability[47] of 10^{-3} for the photoexcited electrons) with a conservatively estimated upper limit of $N_{max} = 2.5 \times 10^{12}$ cm^{-2} (detection probability of 10^{-4}). Considering that at these low coverages only 50–80% of the template is covered by crystallites,[48] the upper limit for the local trap density amounts to $n_{max} = 5 \times 10^{12}$ cm^{-2}. As discussed below, these electrons are bound with respect to the vacuum and localized at the vacuum interface of the crystallites. This makes them ideal candidates for the study of DEA at ice−vacuum interfaces as detailed further below.

3. Solvation and Relaxation from Femtoseconds to Minutes

The long lifetime of the trapped electrons can be utilized to monitor their relaxation dynamics and perform a pump−probe experiment on minute time scales. After illumination of the sample with UV light for 10 s, the photostationary state is established and, resulting from the fluence used, the electrons in the e_T state are on average $\tau_r = 0.1$ s "old", as discussed above. The corresponding 2PPE spectrum is depicted in Figure 3a. To probe the relaxation dynamics at later times, the sample is left unperturbed (no incident photons) and the evolution of the transient e_T population monitored by photoemission with $h\nu_{VIS}$ after the time delay of interest. The respective spectra at $\Delta t = 1$, 10, 60, 300, and 630 s are also shown in Figure 3a. The peak maximum of e_T keeps shifting toward lower energies as time proceeds and as highlighted by the dashed curve (guide to the eye). This energetic shift of the trapped electron feature e_T already starts on femtosecond time scales[41] right after photoinjection via the image potential state. It is a result of a continuing reorganization of the D_2O environment that accommodates the excess charge and relaxes toward equilibrium.

The remarkable observation of an ongoing relaxation over 17 orders of magnitude in time is summarized in Figure 3b, which depicts the energetic shift of the e_T peak maximum as a
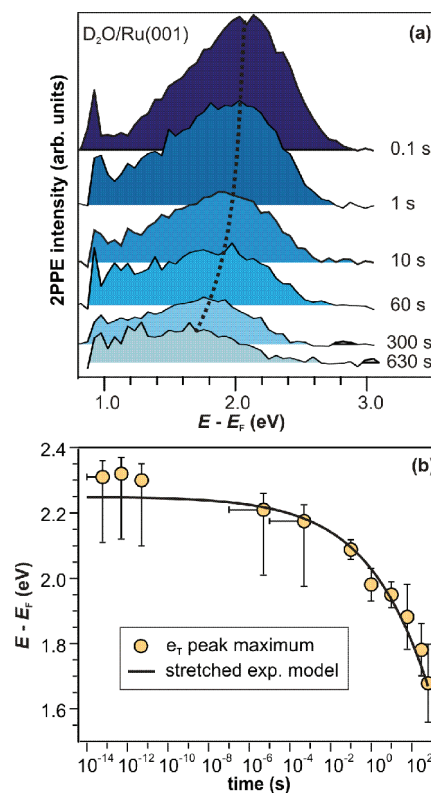

FIGURE 3. (a) 2PPE spectra of the trapped electron feature at various times after excitation. (Ref 42 reproduced by permission of The Royal Society of Chemistry, http://www.rsc.org/). (b) Relaxation dynamics of trapped electrons at supported D_2O crystallites ranging over 17 orders of magnitude in time. Circles denote the position of the e_T peak maximum. The solid line results from a model calculation based on a stretched exponential approach. (Modified with permission from ref 41. Copyright 2009 American Chemical Society.)

function of time after photoexcitation of the trapped electrons. Spanning these many time scales, it can be described in terms of a stretched exponential law (solid line), which results from the distribution of different trapping sites in the sample and their respective characteristic relaxation times, as detailed in ref 42.

One necessary condition for the reactivity of the trapped electrons is the possibility to interact with the reactants (i.e., molecules impinging from the gas phase), which means in the present context their proximity to the vacuum interface. As shown by xenon titration experiments in refs 41 and 49, this is fulfilled: The spectral signature of the trapped electrons, e_T, is quenched when adsorbing Xe atoms onto the supported D_2O crystallites. The rare gas apparently strongly interacts with the electron density in the traps and probably blocks them or strongly reduces the electron lifetimes. As the rare gas does not penetrate into the D_2O bulk, this shows that the e_T electrons must be localized at the vacuum interface of the crystallites.
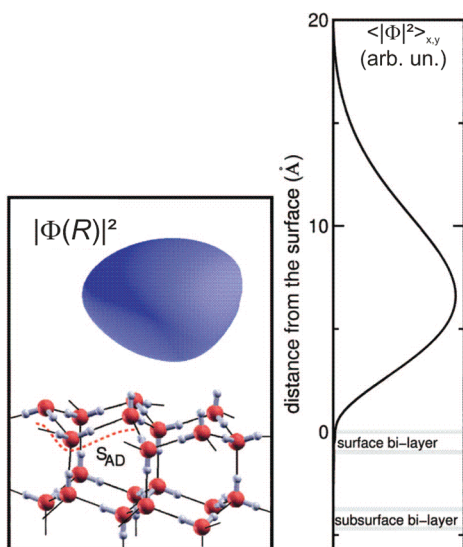
FIGURE 4. Possible trapping site at a crystalline ice surface defect from ab initio calculations. The electron is shown at 70% of its maximum charge density (left). Its overlap even with the topmost ice layer is negligible (right). Adapted with permission from ref 41. Copyright 2009 American Chemical Society.

Possible trapping sites are orientational defects at the ice surfaces as suggested by ab initio density functional theory calculations.[41] Already slight modifications (e.g., flip rotations) of the two topmost bilayers can lead to stabilization of the charge density $|\Phi(R)|^2$ as exemplarily shown in Figure 4. Such reconfigurations of the hydrogen-bonded network lead to a very efficient reduction of the charge density already in the outermost ice layer and provide a theoretical explanation for the long lifetimes accompanied by electronic decoupling of the electron from the metal substrate.

4. Reactivity of Surface Trapped Electrons

It is well-known, that low-energy electrons can efficiently induce chemical reactions by formation of transient negative ions resonances leading to dissociative electron attachment (DEA) processes.[50] In the condensed phase such transient negative ions are energetically stabilized due to polarization (or solvation) of the molecular environment (leading to a downshift of the corresponding potential energy surface, cf. Figure 5a), which may enhance the efficiency of DEA processes. In part, this arises from changes of the energetics of the DEA process; however, the electron dynamics and competing relaxation processes are also critical for the observed reactivity. As the trapped electrons on supported ice crystallites discussed before exhibit lifetimes up to minutes and are bound at the ice vacuum interface, they may thus stimulate electron-induced reactions with molecules coadsorbed on the ice surface or impinging from the gas phase.
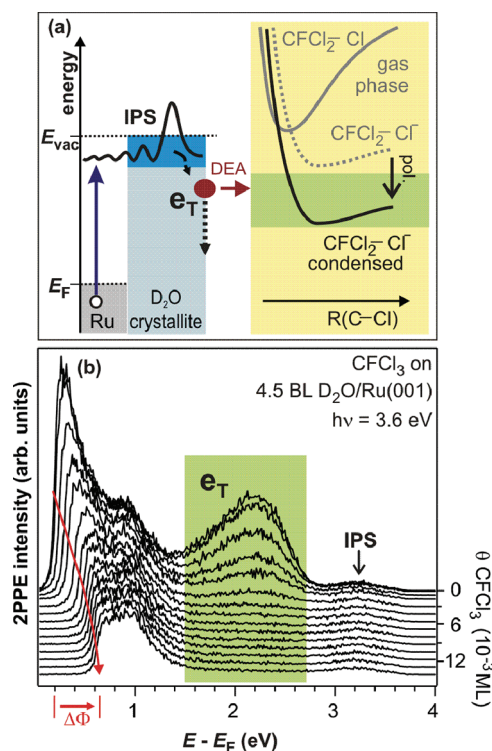

FIGURE 5. (a) Scheme of the DEA reaction of $CFCl_3$ with trapped electrons at the vacuum interface of supported D_2O crystallites. Electrons are created by charge injection via the IPS as discussed above. The Franck−Condon potential of $CFCl_3$ is shifted to lower energies from its gas phase value due to polarization and becomes resonant with trapped electron states (green area), enabling DEA from trapped electrons at the supported ice crystallites. (b) 2PPE spectra recorded with $h\nu = 3.6$ eV from D_2O crystallites on Ru(001) (nominal coverage 4.5 bilayers) as a function of exposure to $CFCl_3$ at 30 K. The spectrum of the freshly prepared crystalline D_2O layer (before $CFCl_3$ adsorption) exhibits a pronounced resonance at $E − E_F = 2.3$ eV due to trapped electrons (e_T). The depletion of this feature by adsorption of small amounts of $CFCl_3$ (<1% of a ML) is accompanied by a work function increase up to $\Delta\Phi = +500$ meV. (Ref 49 reproduced by permission of The Royal Society of Chemistry, http://www.rsc.org/).

Reactions of trapped electrons at ice crystallites with CFCs or oxygen species are of particular interest, because of their potential role in atmospheric ozone depletion.[2−4] In this scenario, the depletion is caused by the release of chlorine, which may originate either from direct photolysis or from DEA of CFCs by capture of electrons produced by cosmic rays in ice particles in polar stratospheric clouds. Even for a small density of low-energy electrons the latter process can dominate, as the DEA cross section often exceeds the photodissociation cross section by several orders of magnitude (e.g., 10^4 times for $CFCl_3$[51]).

In the following, we discuss the reaction of trapped electrons on water-ice crystallites with $CFCl_3$ coadsorbed at the ice surface.[49] Figure 5b shows 2PPE spectra of trapped

electrons at ice crystallites during exposure to CFCl$_3$ at low temperature (30 K). The nominal coverage of CFCl$_3$ θ of the respective spectrum is shown on the right axis. It is remarkable that even for an extremely small coverage of 4×10^{-3} ML of CFCl$_3$ ($\theta_{crit} = 3 \times 10^{12}$ cm^{-2}), the e$_T$ population is quenched in the 2PPE spectra, which is accompanied by a substantial increase of the work function of $\Delta\Phi = +250$ meV. As it is wellknown and widely accepted that DEA processes are induced by low-energy electrons, we assign these observations to dissociative electron attachment of the long-living trapped electrons to coadsorbed CFCl$_3$ molecules, leading to the formation of •CFCl$_2$ radicals and Cl$^-$ anions at the ice surface and the accumulation of negative surface charge.[49,52] The work function change saturates at $\Delta\Phi = +500$ meV upon further CFCl$_3$ exposure.

A key question in this context is the reactivity of each trapping site and the cross section for DEA of adsorbed CFCl$_3$. As discussed in a recent review,[3] the presence of ice enhances the DEA cross section by several orders of magnitude depending on the CFC and leads, in the case of CFCl$_3$, to a cross section of 10^{-13} cm^2. This is equal to the detection limit of the electron trapping technique used for ice and CFCl$_3$ adsorbed on rare gas buffer layers. In the present approach, we inject the electrons from the substrate, rather than from the vacuum, to the pre-existing surface traps described above. Related to studies discussed in ref 3, we define the DEA cross section as

$$\sigma = \frac{r}{N \cdot \theta} \tag{1}$$

with the number of reactions per area r, the trap density N, and the relative CFC coverage θ. This cross section can be understood as the characteristic "active area" of each trap. Based on the analysis of the above-described experiment (Figure 5b) we draw the following conclusions:

(i) The e$_T$ signal is completely quenched for $\theta_{crit} = 3 \times 10^{12}$ cm^{-2}; that is, every trap has interacted with at least one CFCl$_3$ molecule: $r/N \geq 1$. This results in a lower limit $\sigma \geq 1/3 \times 10^{-12}$ cm^2.

(ii) The maximum number of reactions is determined by the number of reactants: $r/\theta_{crit} \leq 1$ with the above estimated trap density $N = 2.5 \times 10^{11}$ cm^{-2} this yields $\sigma \leq 4 \times 10^{-12}$ cm^2.

In addition to these estimations for the upper and lower limit of the trap DEA cross section, however, the measurement of the work function change with and without CFCl$_3$ coadsorption results in a completely independent estimation of the DEA cross section:

(iii) Upon adsorption of θ_{crit}, the work function increases by $\Delta\Phi = 500$ meV. However, pure population of the traps with electrons leads to $\Delta\Phi = 50$ meV. Assuming similar screening of the trapped electrons and Cl$^-$ ions at the ice surface (which is plausible due to similar extension of the charge distribution), at each trap on average 10 molecules would dissociate resulting in a cross section of $\sigma \leq 3 \times 10^{-12}$ cm^2 which lies well within the above derived interval.

The cross section evaluated from these experiments is 2 orders of magnitude larger than the corresponding DEA cross section in the gas[51] and condensed phase[3] without the catalyst ice. This very high cross section and reactivity of trapped electrons at the supported ice crystallites for DEA of CFCl$_3$ can be rationalized by the downshift of the negative ion potential energy surface due to polarization at the crystalline ice surface (see Figure 5a). This brings the Franck–Condon window into resonance with the trapped electron energy distribution (see green shaded area) which strongly enhances the efficiency of DEA processes. Very similar consideration will also apply to other CFCs. These results clearly demonstrate the high reactivity of localized excess electrons trapped at the surface of ice crystallites with electronegative molecular adsorbates. As the dissociation of CFCs on stratospheric ice particles is believed to play a key role in the ozone layer depletion, the long-lived excess electrons discussed in this work may be an important reaction intermediate in atmospheric chemistry.

BIOGRAPHICAL INFORMATION

Julia Stähler received her Ph.D. degree in 2007 with M. Wolf at the Department of Physics of the Freie Universität Berlin. In 2008, she went to the University of Oxford with the Feodor Lynen fellowship of the Humboldt Foundation to work as a postdoc in the group of Andrea Cavalleri. In 2009, she became the group leader of the electron dynamiχ group at the Fritz Haber Institute of the Max Planck Society (Department of Physical Chemistry).

Cornelius Gahl is a senior scientist in the group of Martin Weinelt since 2006, currently moving from the Max-Born-Institute in Berlin to

the Department of Physics of the Freie Universität Berlin. There, he already received his Ph.D. degree in 2004 with M. Wolf. His work is dedicated to electronic excitations and spectroscopy of molecules at surfaces.

Martin Wolf is director of the Department of Physical Chemistry at the Fritz Haber Institute of the Max Planck Society in Berlin since 2008. He received his Ph.D. degree in 1991 from the Freie Universität Berlin (supervisor Gerhard Ertl). After a postdoctoral period in Austin, Texas, with Mike White, he set up a laboratory for femtosecond surface spectroscopy at the Fritz-Haber-Institute and was also a visiting scientist at IBM Yorktown Heights with Tony Heinz. In 2000, he was appointed as a Full Professor for Experimental Physics at the Freie Universität Berlin.

REFERENCES

1 Garrett, B. C.; Dixon, D. A.; Camaioni, D. M.; Chipman, D. M.; Johnson, M. A.; Jonah, C. D.; Kimmel, G. A.; Miller, J. H.; Rescigno, T. N.; Rossky, P. J.; Xantheas, S. S.; Colson, S. D.; Laufer, A. H.; Ray, D. R.; Barbara, P. F.; Bartels, D. M.; Becker, K. H.; Bowen, K. H.; Bradforth, S. E.; Carmichael, I.; Coe, J. V.; Corrales, L. R.; Cowin, J. P.; Dupuis, M.; Eisenthal, K. B.; Franz, J. A.; Gutowski, M. S.; Jordan, K. D.; Kay, B. D.; LaVerne, J. A.; Lymar, S. V.; Madey, T. E.; McCurdy, C. W.; Meisel, D.; Mukamel, S.; Nilsson, A. R.; Orlando, T. M.; Petrik, N. G.; Pimblott, S. M.; Rustad, J. R.; Schenter, G. K.; Singer, S. J.; Tokmakoff, A.; Wang, L.-S.; Zwier, T. S. Role of Water in Electron-Initiated Processes and Radical Chemistry: Issues and Scientific Advances. *Chem. Rev.* **2005**, *105*, 355–390.

2 Prather, M. J.; Watson, R. T. Stratospheric ozone depletion and future levels of atmospheric chlorine and bromine. *Nature* **1990**, *344*, 729–734.

3 Lu, Q.-B. Cosmic-ray-driven electron-induced reactions of halogenated molecules adsorbed on ice surfaces: Implications for atmospheric ozone depletion and global climate change. *Phys. Rep.* **2010**, *487*, 141–167.

4 Grooß, J.-U.; Müller, R. Do cosmic-ray-driven electron-induced reactions impact stratospheric ozone depletion and global climate change? *Atmos. Environ.* **2011**, *45*, 3508–3514.

5 Marin, T. W.; Takahashi, K.; Jonah, C. D.; Chemerisov, S. D.; Bartels, D. M. Recombination of the hydrated electron at high temperature and pressure in hydrogenated alkaline water. *J. Phys. Chem. A* **2007**, *111*, 11540–51.

6 Kevan, L. Solvated electron structure in glassy matrixes. *Acc. Chem. Res.* **1981**, *14*, 138–145.

7 Marsalek, O.; Uhlig, F.; Frigato, T.; Schmidt, B.; Jungwirth, P. Dynamics of Electron Localization in Warm versus Cold Water Clusters. *Phys. Rev. Lett.* **2010**, *105*, 043002-1–4.

8 Larsen, R.; Glover, W. J.; Schwartz, B. J. Does the Hydrated Electron Occupy a Cavity? *Science* **2010**, *329*, 65–69.

9 Jordan, K. D.; Johnson, M. A. Downsizing the Hydrated Electron's Lair. *Science* **2010**, *329*, 42.

10 Turi, L.; Madarász, Á. Comment on "Does the Hydrated Electron Occupy a Cavity? *Science* **2011**, *331*, 1387.3.

11 Jacobson, L. D.; Herbert, J. M. Comment on "Does the Hydrated Electron Occupy a Cavity? *Science* **2011**, *331*, 1387.4.

12 Larsen, R. E.; Glover, W. J.; Schwartz, B. J. Response to comments on "Does the Hydrated Electron Occupy a Cavity? *Science* **2011**, *331*, 1387.5.

13 Barnett, R. N.; Landman, U.; Cleveland, C. L.; Jortner, J. Electron localization in water clusters. II. Surface and internal states. *J. Chem. Phys.* **1988**, *88*, 4429–4447.

14 Coe, J. V.; Lee, G. H.; Eaton, J. G.; Arnold, S. T.; Sarkas, H. W.; Bowen, K. H.; Ludewigt, C.; Haberland, H.; Worsnop, D. R. Photoelectron spectroscopy of hydrated electron cluster anions, $(H_2O)^-_{n=2-69}$. *J. Chem. Phys.* **1990**, *92*, 3980–3982.

15 Paik, D. H.; Lee, I.-R.; Yang, D.-S.; Baskin, J. S.; Zewail, A. H. Electrons in Finite-Sized Water Cavities: Hydration Dynamics Observed in Real Time. *Science* **2004**, *306*, 672–675.

16 Jordan, K. D. A Fresh Look at Electron Hydration. *Science* **2004**, *306*, 618–619.

17 Bragg, A. E.; Verlet, J. R. R.; Kammrath, A.; Cheshnovsky, O.; Neumark, D. M. Hydrated Electron Dynamics: From Clusters to Bulk. *Science* **2004**, *306*, 669–671.

18 Madarasz, A.; Rossky, P. J.; Turi, L. Interior- and surface-bound excess electron states in large water cluster anions. *J. Chem. Phys.* **2009**, *130* (12), 124319-1–7.

19 Li, B.; Zhao, J.; Onda, K.; Jordan, K. D.; Yang, J.; Petek, H. Ultrafast Interfacial Proton-Coupled Electron Transfer. *Science* **2006**, *311*, 1436–1440.

20 Gahl, C.; Bovensiepen, U.; Frischkorn, C.; Wolf, M. Ultrafast Dynamics of Electron Localization and Solvation in Ice Layers on Cu(111). *Phys. Rev. Lett.* **2002**, *89*, 107402-1–4.

21 Zhao, J.; Li, B.; Onda, K.; Feng, M.; Petek, H. Solvated Electrons on Metal Oxide Surfaces. *Chem. Rev.* **2006**, *106*, 4402–4427.

22 Stähler, J.; Mehlhorn, M.; Bovensiepen, U.; Meyer, M.; Kusmierek, D. O.; Morgenstern, K.; Wolf, M. Impact of ice structure on ultrafast electron dynamics in D_2O clusters on Cu(111). *Phys. Rev. Lett.* **2007**, *98*, 206105-1–4.

23 Meyer, M.; Stähler, J.; Kusmierek, D. O.; Wolf, M.; Bovensiepen, U. Determination of the electron's solvation site on D_2O/Cu(111) using Xe overlayers and femtosecond photoelectron spectroscopy. *Phys. Chem. Chem. Phys.* **2008**, *10*, 4932–4938.

24 Hodgson, A.; Haq, S. Water adsorption and the wetting of metal surfaces. *Surf. Sci. Rep.* **2009**, *64*, 381–451.

25 Mehlhorn, M.; Morgenstern, K. Faceting during the Transformation of Amorphous to Crystalline Ice. *Phys. Rev. Lett.* **2007**, *99*, 246101-1–4.

26 Kimmel, G. A.; Petrik, N. G.; Dohnalek, Z.; Kay, B. D. Layer-by-layer growth of thin amorphous solid water films on Pt(111) and Pd(111). *J. Chem. Phys.* **2006**, *125*, 044713-1–12.

27 Kimmel, G. A.; Petrik, N. G.; Dohnalek, Z.; Kay, B. D. Crystalline Ice Growth on Pt(111): Observation of a Hydrophobic Water Monolayer. *Phys. Rev. Lett.* **2005**, *95*, 166102-1–4.

28 Lu, Q. B.; Sanche, L. Enhanced Dissociative Electron Attachment to CF_2Cl_2 by Transfer of Electrons in Precursors to the Solvated State in Water and Ammonia Ice. *Phys. Rev. B* **2001**, *63*, 153403-1–4.

29 Ryu, S.; Chang, J.; Kwon, H.; Kim, S. K. Dynamics of Solvated Electron Transfer in Thin Ice Film Leading to a Large Enhancement of Photodissection of $CFCl_3$. *J. Am. Chem. Soc.* **2006**, *128*, 3500–3501.

30 Griffin, G. B.; Young, R. M.; Ehrler, O. T.; Neumark, D. M. Electronic relaxation dynamics in large anionic water clusters: $(H_2O)_n^-$ and $(D_2O)_n^-$ (n = 25–200). *J. Chem. Phys.* **2009**, *131*, 194302-1–9.

31 Frigato, T.; Vondele, J. V.; Schmidt, B.; Schütte, C.; Jungwirth, P. Ab Initio Molecular Dynamics Simulation of a Medium-Sized Water Cluster Anion: From an Interior to a SurfaceLocated Excess Electron via a Delocalized State. *J. Phys. Chem. A* **2008**, *112*, 6125–6133.

32 Alfano, J. C.; Walhout, P. K.; Kimura, Y.; Barbara, P. F. Ultrafast transient-absorption spectroscopy of the aqueous solvated electron. *J. Chem. Phys.* **1993**, *98* (7), 5996–5998.

33 Siefermann, K. R.; Liu, Y.; Lugovoy, E.; Link, O.; Faubel, M.; Buck, U.; Winter, B.; Abel, B. Binding energies, lifetimes and implications of bulk and interface solvated electrons in water. *Nat. Chem.* **2010**, *2*, 274–279.

34 Shreve, A. T.; Yen, T. A.; Neumark, D. M. Photoelectron spectroscopy of hydrated electrons. *Chem. Phys. Lett.* **2010**, *493*, 216–219.

35 Assel, M.; Laenen, R.; Laubereau, A. Retrapping and solvation dynamics after femtosecond UV excitation of the solvated electron in water. *J. Chem. Phys.* **1999**, *111*, 6869–6874.

36 Migus, A.; Gauduel, Y.; Martin, J. L.; Antonetti, A. Excess electrons in liquid water: First evidence of a prehydrated state with femtosecond lifetime. *Phys. Rev. Lett.* **1987**, *58*, 1559–1562.

37 Johns, J. E.; Muller, E. A.; Fréchet, J. M. J.; Harris, C. B. The Origin of Charge Localization Observed in Organic Photovoltaic Materials. *J. Am. Chem. Soc.* **2010**, *132*, 15720–15725.

38 Zhu, X.-Y.; Yang, Q.; Muntwiler, M. Charge-Transfer Excitons at Organic Semiconductor Surfaces and Interfaces. *Acc. Chem. Res.* **2009**, *42*, 1779–1787.

39 Ge, N.-H.; Wong, C. M.; Lingle, R. L., Jr.; McNeill, J. D.; Gaffney, K. J.; Harris, C. B. Femtosecond Dynamics of Electron Localization at Interfaces. *Science* **1998**, *279*, 202–205.

40 Stähler, J.; Meyer, M.; Kusmierek, D. O.; Bovensiepen, U.; Wolf, M. Ultrafast electron transfer dynamics at NH_3/Cu(111) interfaces: Determination of the transient tunneling barrier. *J. Am. Chem. Soc.* **2008**, *130* (27), 8797–8803.

41 Bovensiepen, U.; Gahl, C.; Stähler, J.; Bockstedte, M.; Meyer, M.; Baletto, F.; Scandolo, S.; Zhu, X.-Y.; Rubio, A.; Wolf, M. A Dynamic Landscape from Femtoseconds to Minutes for Excess Electrons at Ice—Metal Interfaces. *J. Phys. Chem. C* **2009**, *113*, 979–988.

42 Stähler, J.; Meyer, M.; Bovensiepen, U.; Wolf, M. Solvation dynamics of surface-trapped electrons at NH_3 and D_2O crystallites adsorbed on metals: From femtosecond to minute timescales. *Chem. Sci.* **2011**, *2* (5), 907–916.

43 We use D_2O instead of H_2O because of the lower background pressure at m = 20 for thermal desorption spectroscopy and coverage determination. The spectroscopic and time-dependent observations are qualitatively the same for both isotopes.

44 Bovensiepen, U.; Gahl, C.; Wolf, M. Solvation Dynamics and Evolution of the Spatial Extent of Photoinjected Electrons in D_2O/Cu(111). *J. Phys. Chem. B* **2003**, *107*, 8706–8715.

45 Gahl, C. Elektronentransfer- und Solvatisierungsdynamik in Eis adsorbiert auf Metalloberflächen. Ph.D. Thesis, Freie Universität Berlin, Germany, 2004, http://www.diss.fu-berlin.de/diss/receive/FUDISS_thesis_000000001387

46 Stähler, J. Freezing Hot Electrons - Electron Transfer and Solvation Dynamics at D_2O- and NH_3-Metal Interfaces. Ph.D. Thesis, Freie Universität Berlin, Germany, 2007, http://www.diss.fu-berlin.de/diss/receive/FUDISS_thesis_000000002622

47 This estimate is based on the spectrometer opening angle of 3.8°, the assumption of a cosine-like emission of the trapped electrons, and the detection sensitivity of the channel plates.

48 Haq, S.; Hodgson, A. Multilayer Growth and Wetting of Ru(0001). *J. Phys. Chem.* **2007**, *111*, 5946–5953.

49 Bertin, M.; Meyer, M.; Stähler, J.; Gahl, C.; Wolf, M.; Bovensiepen, U. Reactivity of water-electron complexes on crystalline ice surfaces. *Faraday Discuss.* **2009**, *141*, 293–307.

50 Bass, A. D.; Sanche, L. Reactions induced by low energy electrons in cryogenic films. *Low Temp. Phys.* **2003**, *29*, 202–214.

51 Illenberger, E.; Scheunemann, H.-U.; Baumgärtel, H. Negative ion formation in CF_2Cl_2, CF_3Cl, and $CFCl_3$ following low energy (0—10 eV) impact with near monoenergetic electrons. *Chem. Phys.* **1979**, *37*, 21–31.

52 It was not possible to detect either product using the quadrupole mass spectrometer. The coverage is with 3×10^{-12} cm^{-2} very low and the products might migrate through the ice and desorb from the metal template at elevated temperatures or even further react with the D_2O.